4
Effect of precursors on CZTS thin film prepared using Sol-gel spin coating

4.1 Introduction

Deposition of sulfur based quaternary chacogenide CZTS is a bit difficult in its most stable kesterite phase without impurities, which is very important because of its numerous applications such as a counter electrode in dye-sensitized solar cell (DSSC) [Xin, He, Han, Jung, & Lin, 2011][Dai et al., 2012], photocatalyst for hydrogen production [Yu et al., 2015],[J. Wang, Zhang, Song, & Gao, 2014],[Jiang et al., 2015] and as a gas sensor [Gurav et al., 2014][Shinde, Deshmukh, Patil, & Lokhande, 2013]. Sol gel process is a wet chemical process where a stable colloidal suspension (sol) is first formed and then gelation of the sol is done to form a network in continuous liquid phase (gel). Ageing is needed to convert sol into a gel. This process is also called as Oswald ageing process and is very important to control the microscopic properties of the grown material. In gel the solid particles are encapsulated with the solvent. The viscosity of gel is tailored to make it suitable for spin coating. The solvent after spin coating the gel on the substrate is usually removed by evaporating during the drying step at elevated temperature. The drying process significantly influences the microscopy of the formed film. In fact all the experimental parameter even seemingly unimportant plays a significant role in formation and characteristics of the grown film.

Spin coating and drying processes are followed several times to get desired thickness of the film. During drying solvent is evaporated from the gel. This increases capillary pressure associated with liquid vapor interface within a pore. For a pore of radius r capillary pressure can be given by $P = \frac{2\gamma \cos\alpha}{r}$, where P is capillary pressure, γ is surface tension, r is pore radius and α is contact angle between liquid and solid [Soler-Illia, 2009]. A high temperature gradient during drying can result in large capillary pressure in such pores which may lead to the collapse of pores and finally degrade the film quality. The capillary pressure can also be reduced by selecting a solvent with lower surface tension and contact angle close to 90 degree [Mattox, 1998]. Sol-gel technique is a very low cost and simple solution for fabricating thin films and has industrial applications in making numerous products [W. Li & Seal, 2004]. This present chapter explores sol-gel spin coating technique for the CZTS growth. Chloride and nitrate salts are chosen and their chemistry is discussed during the sol formation. The selectivity and suitability of precursor for spin coating are discussed with their impact on morphological, optical and electronic properties, of the deposited thin film which may be useful for their applications mainly in solar photovoltaic.

4.2 Formation of CZTS sol for spin coating

We started with two set of precursors to form sol-gel suitable for the coating: 1) chloride based precursors, calling chloride route and 2) Nitrate precursors, calling nitrate route in later discussions. In chloride precursor solution, chloride salts of Cu, Zn and Sn are taken in the compositional ratio of 2 : 1 : 1 : 8. 0.04 M Copper (II) chloride dihydrate ($CuCl_2.2H_2O$, ≥ 99% Alfa Aesar), 0.02M anhydrous zinc chloride ($ZnCl_2$, ≥ 98% Alfa Aesar) and 0.02M Tin(II) chloride ($SnCl_2.2H_2O$, ≥ 98%, Sigma Aldrich) are dissolved successively under continuous stirring in 2 methoxy ethanol with 50 ppm butylhydroxytoluene (BHT) used as a stabilizer. At

least 5 min wait time is given in between the dissolution of each metal salts. At the end 0.16 M thiourea ($(NH_2)_2CS$, ≥ 99% Himedia) is mixed in the solution as sulfur source and kept the solution on stirring and ageing for 1 hour.

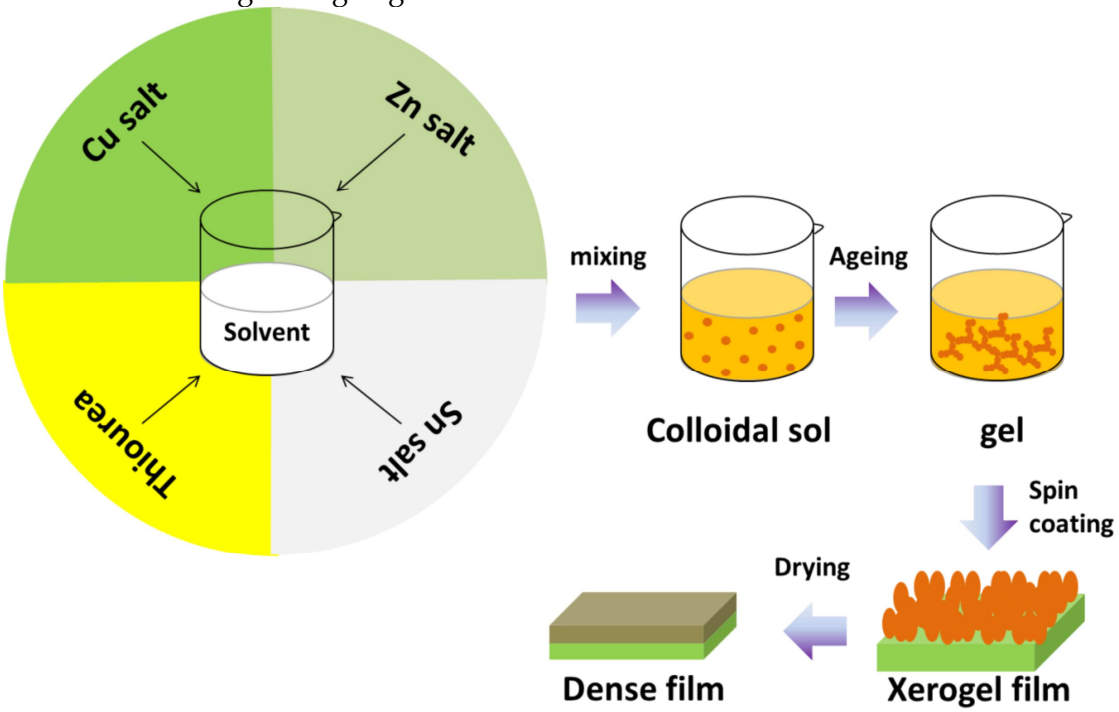

Figure 4.1 Schematic representation of process of formation of CZTS thin film

During this process initial dark green color of copper chloride solution turns into the light green after adding zinc chloride, which after dissolution of tin chloride turned into transparent milky white solution. Formation of CZTS sol starts after dissolution of thiourea in the reaction mixture. This process is schematically represented in **Figure 4.1**. With ageing metal-thiourea complexes are formed and the solution finally turns into a yellow colored transparent sol which contains metal ions and metal-thiourea complex. Excess of thiourea is used in the synthesis of CZTS sol for two reasons. First, it helps in the formation of stable sol, which is essential for spin coating and secondly it avoids the sulfur loss during post thermal treatment of the pristine spin coating of thin films. Several attempts were made with different solvents such as methanol, ethanol and DI water and none of them resulted in a stable sol and the solution was precipitating after some time. Further, 2-methoxyethanol resulted in stable sol because of its polar nature and the sol was stable over several months. This 2-methoxyethanol based stable sol is used for preparing CZTS sol to fabricate CZTS thin films using spin coating.

In a different approach nitrate salts of Cu and Zn are utilized to prepare CZTS sol. Copper(II) nitrate hemi-pentahydrate ($CuN_2O_6.5H_2O$), zinc nitrate hexahydrate ($N_2O_6Zn.6H_2O$), stannous chloride ($SnCl_2.2H_2O$) and thiourea (CH_4N_2S) were dissolved successively in 2 methoxy ethanol solvent in the desired molar ratio of Cu : Zn : Sn : S :: 2 : 1 : 1 : 4 to form a stable CZTS sol. Here, in nitrate precursor's route, the desired molar ratio of thiourea was sufficient to synthesize a stable sol. The probable chemical processes are summarized in **Table 4.1**. Any attempt with excess thiourea resulted in a stable sol solution, however, the prepared films shows poor adherence to the substrate and hence excess thiourea is discarded for nitrate precursors. CZTS sol prepared using both chloride and nitrate precursors are acidic in nature and pH values are ~ 0.3 and ~ 0.1, respectively. The probable reaction chemistry governing the formation of CZTS sols in both the routes are summarized in **Table 4.1**

Table 4.1 Probable reaction path for CZTS formation

chloride route	nitrate route
$Cu(Cl)_2 \rightarrow Cu^{2+} + 2Cl^-$ $Zn(Cl)_2 \rightarrow Zn^{2+} + 2Cl^-$ $SnCl_2 \rightarrow Sn^{2+} + 2Cl^-$ $(NH_2)_2CS \rightarrow NH_2\text{-}C^+\text{=}NH + H^+ + S^{2-}$ $2Cu^{2+} + Zn^{2+} + Sn^{2+} + 4S^{2-} \rightarrow Cu_2ZnSnS_4$ $2Cu(Cl)_2.2H_2O + Zn(Cl)_2 + SnCl_2.2H_2O + 4(NH_2)_2CS + 8H_2O \rightarrow Cu_2ZnSnS_4 + 8NH_4Cl + 4CO_2$	$Cu(NO_3)_2 \rightarrow Cu^{2+} + 2NO_3^-$ $Zn(NO_3)_2 \rightarrow Zn^{2+} + 2NO_3^-$ $SnCl_2 \rightarrow Sn^{2+} + 2Cl^-$ $(NH_2)_2CS \rightarrow NH_2\text{-}C^+\text{=}NH + H^+ + S^{2-}$ $2Cu^{2+} + Zn^{2+} + Sn^{2+} + 4S^{2-} \rightarrow Cu_2ZnSnS_4$ $2Cu(NO_3)_2.5H_2O + Zn(NO_3)_2.6H_2O + SnCl_2.2H_2O + 4CH_4N_2S \rightarrow \mathbf{Cu_2ZnSnS_4} + 6NH_4NO_3 + 2NH_4Cl + 4CO_2 + 5H_2O$

4.3 Deposition of CZTS thin film

CZTS thin films are deposited on 2.5 cm x 2.5 cm SLG substrates. These substrates are first cleaned using the process mentioned in **section 3.1**. Further, CZTS thin film is fabricated by spin coating the prepared CZTS sol on these cleaned SLG substrates at 2600 rpm followed by drying at 250 °C over hot plate in open atmosphere. This process of spin coating is repeated three times to achieve the desired film thickness. CZTS thin films thus prepared are later subjected to final heat treatment at 250 °C, 300 °C and 350 °C over hot plate in air ambient for 30 min.

4.4 Result and Discussion

CZTS films prepared using chloride and nitrate salts are represented as MX and MXN along with their processing temperature. Crystallographic structure of the prepared films are investigated using X-ray diffraction patterns and are summarized in **Figure 4.2** for both MX and MXN films processed at different temperatures.

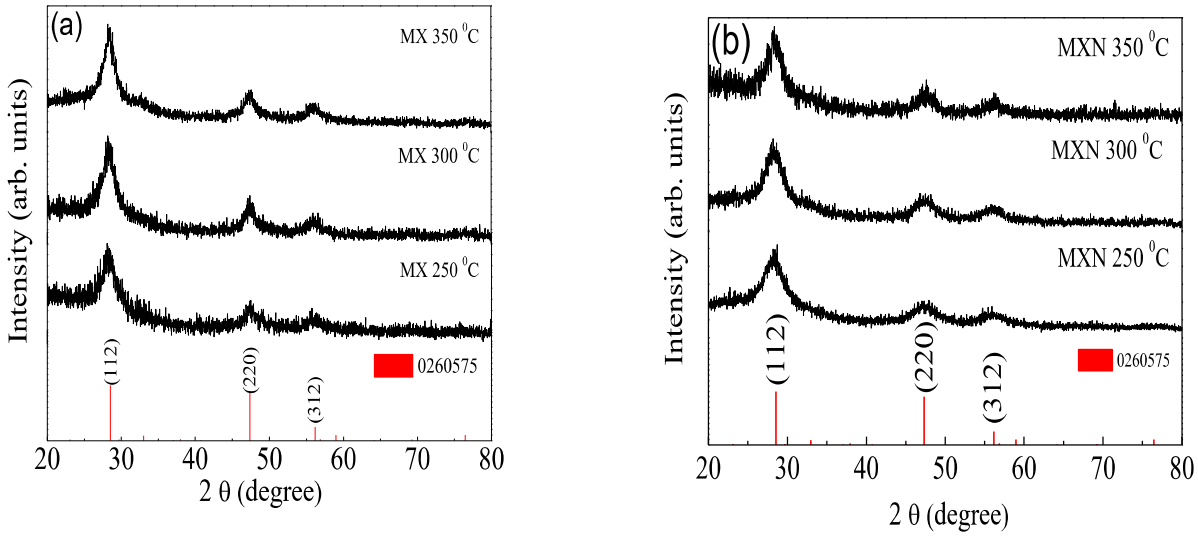

Figure 4.2 XRD micrographs of CZTS thin films at different processing temperatures (a) Chloride precursor route (MX) and (b) Nitrate precursor route (MXN)

X-ray diffraction pattern for the synthesized CZTS thin films are in agreement with the standard crystallographic database ICDD # 026-0575 for kesterite CZTS reference. The observed high intensity peaks at 2θ ~ 28.4°, 47.5° and 56.3° correspond to (112), (220) and (312) crystal planes respectively. The crystal planes are also marked in XRD pattern shown in **Figure 4.2** for easy identification. The obtained XRD results suggest that CZTS films are relatively textured along (1 1 2) plane and the crystallinity improves with increase in annealing temperature. Texture

coefficient (TC (h k l)) for the films has been calculated using the relationship, $TC(h\,k\,l) = \frac{\frac{I\,(h\,k\,l)}{I_0\,(h\,k\,l)}}{N^{-1}\sum\frac{I\,(h\,k\,l)}{I_0\,(h\,k\,l)}}$; where N is the order of reflection, I is measured intensity and I_0 is standard reference intensity taken from ICDD # 026-0575 [Bilgin, Kose, Atay, & Akyuz, 2005]. The grain size (D) of the films is calculated using Scherrer's formula: $Grain\ size = \frac{0.94*\lambda}{B\ Cos\ \theta}$; where B is full width at half maxima (FWHM) of the diffraction peak measured in radians, θ is Bragg's angle of diffraction, and λ is characteristic wavelength of Cu-K_α X-ray incident radiation [Bilgin et al., 2005]. The length of dislocation lines per unit volume or dislocation density, in the prepared film is calculated using Williamsons and Smallman's equation $\delta = \frac{n}{D^2}$; where n is unity for minimum dislocation density and D is the crystallite size [Williamson & Smallman, 1956]. The texture coefficient is summarized in **Figure 4.3** along (112) plane for these CZTS thin films. The (112) textured crystallinity shows better texturing for chloride sol processed films (MX) as compared to nitrate sol prepared CZTS films (MXN).

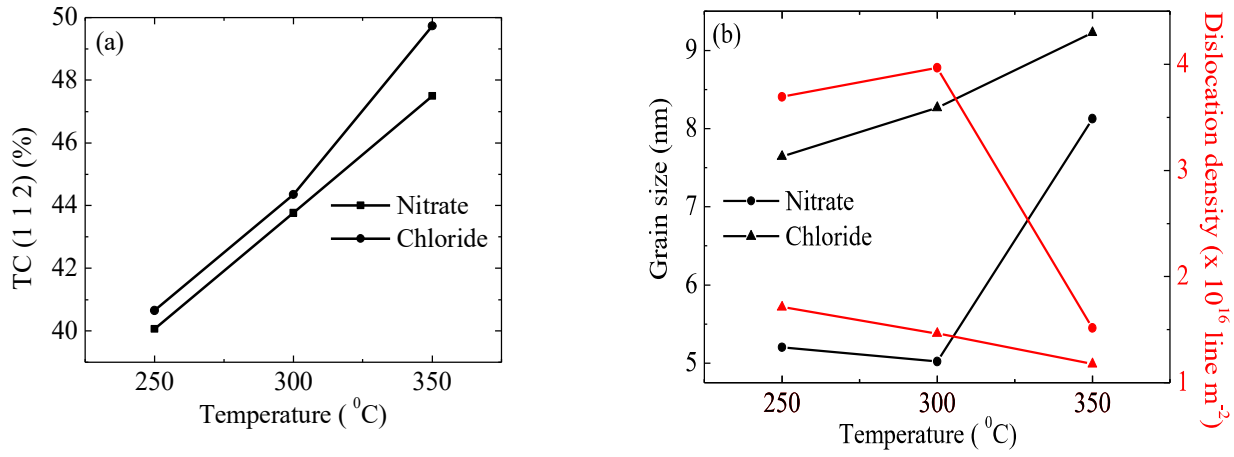

Figure 4.3 (a) Texture coefficient, and (b) Grain size and dislocation density variation with processing temperature for MX and MXN CZTS thin films.

The grain size and dislocation density measured for different CZTS thin films are shown in **Figure 4.3** processed at different temperature and using different sol. It is observed from the measurement that films processed at higher temperature show larger grains for both chloride sol (MX) and nitrate sol (MXN) derived films. We also observed that film prepared using chloride sol always shows larger grains at all processing temperatures compared to film prepared using nitrate sol. The dislocation density shows inverse square characteristics with measured grain size and decreases with increase in processing temperature. Thus, higher processing temperature favors high crystallinity and larger grain growth in CZTS films. In contrary, annealing at higher temperature (> 350 °C) in open atmosphere show adverse effect on the phase purity of the prepared films. This is because of the formation of unwanted oxides and binary and ternary sulfides. Also, the enhanced elemental losses of sulfur and volatile Sn, Zn are observed for annealing beyond 350 °C in open atmosphere.

The strain in prepared CZTS thin films has been calculated using the relation $\varepsilon = \frac{B\ cos\theta}{4}$ and summarized in **Table 4.2**. The stacking fault probability, α, for the layers undergoing stacking fault in the film, defined as $\alpha = \left[\frac{2\pi^2}{45\sqrt{3}tan\theta}\right]\Delta(2\theta)$ where θ is the measured (1 1 2) Bragg's angle. The calculated stacking fault probability corresponding to shift in (112) diffraction peak relative to

reference ICDD# 0260575 in the films are listed in **Table 4.2**. These calculated fault probability values suggest that stacking fault decreases with increase in annealing temperature.

Table 4.2 2θ value for (1 1 2) crystallographic plane, FWHM, average crystallite size, dislocation density, strain, stacking fault probability for CZTS thin film prepared with different routes and different annealing conditions.

Sample	Temperature	2θ for (1 1 2) plane	FWHM	Average Crystallite size (nm)	Dislocation density (δ x 10^{16}) (line m^{-2})	Strain (ε) (line^{-2} m^{-4})	Stacking fault probability (α)
MX	250	28.234	1.72	7.64	1.71	0.417	0.299
	300	28.344	1.70	8.27	1.46	0.411	0.187
	350	28.357	0.88	9.22	1.17	0.213	0.174
MXN	250	28.279	1.66	5.20	3.69	0.402	0.253
	300	28.296	2.08	5.02	3.96	0.504	0.236
	350	28.406	1.40	8.13	1.51	0.337	0.125

To further confirm the phase purity, room temperature Raman spectra are collected for the prepared CZTS thin films, processed at 300 °C using both the sols. The collected Raman spectra are shown in **Figure 4.4**. The presence of an intense vibrational peak at 331 cm^{-1} and two small peaks at ~169 cm^{-1} and 252 cm^{-1} correspond to the characteristics Raman mode for kesterite CZTS. These measured Raman spectra for CZTS also substantiate XRD results for their phase purity and are also in agreement with the previously reported data [Ghediya & Chaudhuri, 2015]. The strongest vibrational mode observed at 331 cm^{-1} is attributed to the local structural inhomogeneity within the disordered cation sublattice and its presence suggests the Cu-poor composition of CZTS material. The observed Raman spectra do not reveal any vibration modes matching to impurity/secondary phases such as CuS (474 cm^{-1}), Cu_2S (472 cm^{-1}) [Minceva-Sukarova, Najdoski, Grozdanov, & Chunnilall, 1997]; ZnS (278, 351 cm^{-1}) [Cheng et al., 2009]; SnS (192 cm^{-1}) [Chandrasekhar, Humphreys, Zwick, & Cardona, 1977], and SnS_2 (205, 315 cm^{-1})[Smith, Meek, & Liang, 1977] binary secondary phases and Cu_2SnS_3 (CTS) (303, 355 cm^{-1} for cubic CTS and 336, 351 cm^{-1} for tetragonal CTS) ternary secondary phases [Fernandes, Salomé, & da Cunha, 2010],[Fernandes, Salomé, & Da Cunha, 2010]. The absence of any impurity/ secondary phases validates the formation of kesterite phase CZTS even at the microscopic level.

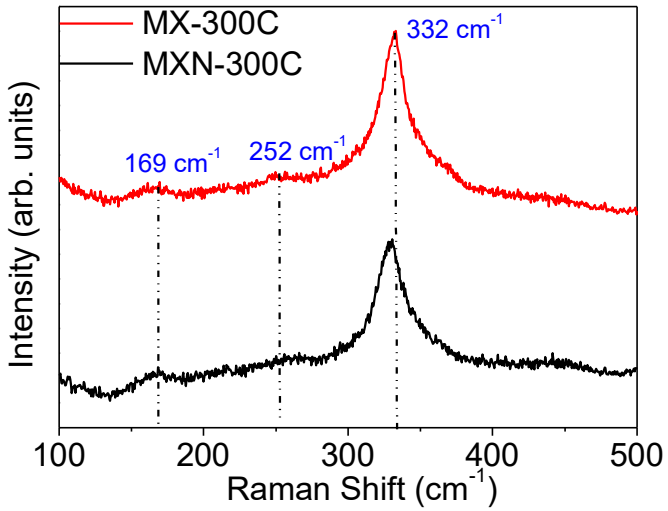

Figure 4.4 Room temperature Raman spectra of 300 °C annealed MX and MXN CZTS thin films.

Elemental composition and the morphology of prepared films have been investigated using energy dispersive X-ray (EDX) and scanning electron microscopy (SEM) measurements. The obtained microscopic results are shown in **Figure 4.5 (a)** for both chloride sol and nitrate sol

derived CZTS film after annealing at 300 °C. The SEM micrograph suggests formation of highly uniform CZTS films using chloride sol **Figure 4.5 (a)** as compared to nitrate sol derived films **Figure 4.5 (b),** which shows presence of large cracks and voids. The observed larger grain with CZTS film processed using chloride sol as compared to that of CZTS film processed using nitrate sol. The results are also in agreement with the XRD results discussed earlier. The schematic representation of the observed surface morphology for the films are shown in **Figure 4.5 (c, d),** representing dense and larger grains for chloride sol derived films while visible voids, cracks and blisters for nitrate sol derived CZTS films. Further, compositional analysis of the films is done at several areas across the film and elemental mapping is done to see the compositional uniformity and elemental distribution in the films. The elemental mapping results are shown in the inset of **Figure 4.5 (a)** for chloride sol prepared CZTS film, showing uniform distribution of constituent elements. In contrast, cracks and voids are clearly visible even at lower magnification for nitrate sol derived CZTS films as shown in inset of **Figure 4.5 (b)**. These films do not show good adherence to the substrate, which is possibly due to the compressive stress or due to the formation of micro bubbles of trapped gases during the synthesis of material which blisters during the time of thermal treatment. This blistering of films is also in consistent with some previous observations [Malerba et al., 2016]. These nitrate sol derived films also consist of smooth regions, which are relatively defect free with smaller grains. The EDAX mapping on the defective region suggests that they are deficient in copper, and tin, as shown in the inset of **Figure 4.5 (b).** In such defective regions, zinc composition is relatively uniform, which suggests the possibility of presence of Zn at the lower surface and loss of volatile Sn and Cu because of their low vapor pressure. However, relatively uniform film composition is observed across smooth areas in the film.

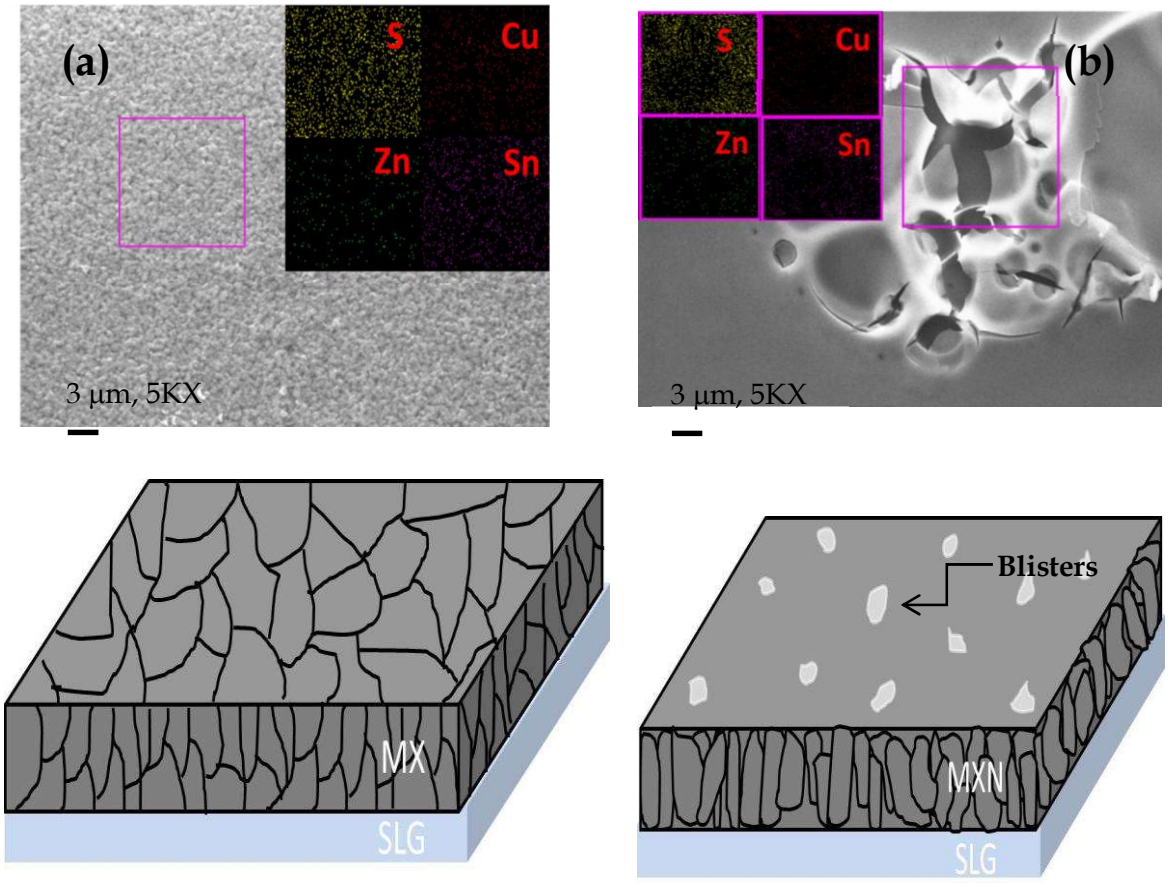

Figure 4.5 Surface SEM micrograph and EDAX mapping (inset) for a) chloride precursor film b) nitrate precursor film and an schematic 3D representation of (c) chloride sol derived CZTS film, showing polycrystalline nature with large grains; (d) nitrate sol derived CZTS film, with blisters at the surface

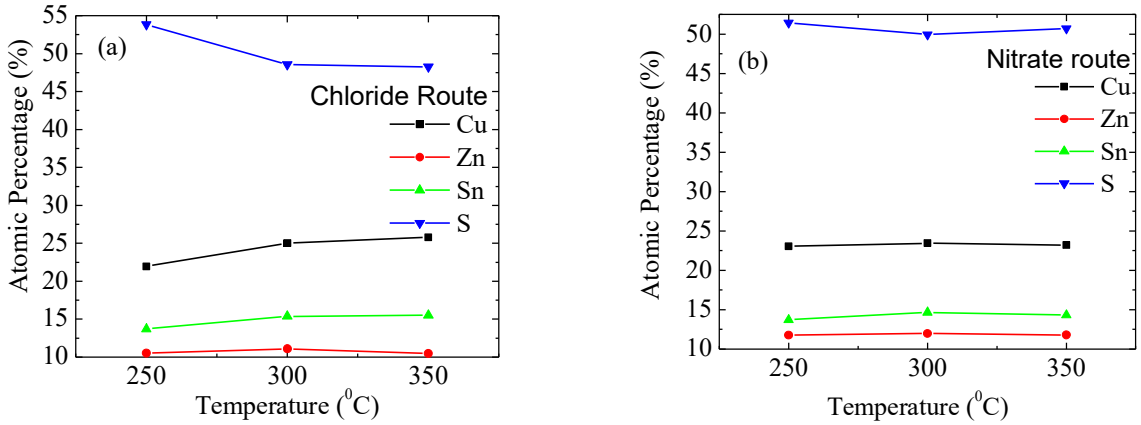

Figure 4.6 EDAX compositional details for CZTS thin films prepared at different annealing temperature using (a) chloride sol (b) Nitrate sol

The details of composition variation with respect to temperature are summarized in **Figure 4.6** for the CZTS film prepared at different temperature using chloride and nitrate sols. We observed that the compositions of these CZTS films are non-stoichiometric and are Cu poor and slightly tin rich in configuration. The cross sectional and surface SEM micrographs are shown in **Figure 4.7 (a, c),** also confirm the formation of uniform, less defective and void free film using chloride sol whereas large cracks are propagated from surface to the back interface and blisters are observed at the surface for films using nitrate sol, as shown in their cross sectional and surface SEM image **Figure 4.7 (c, d).**

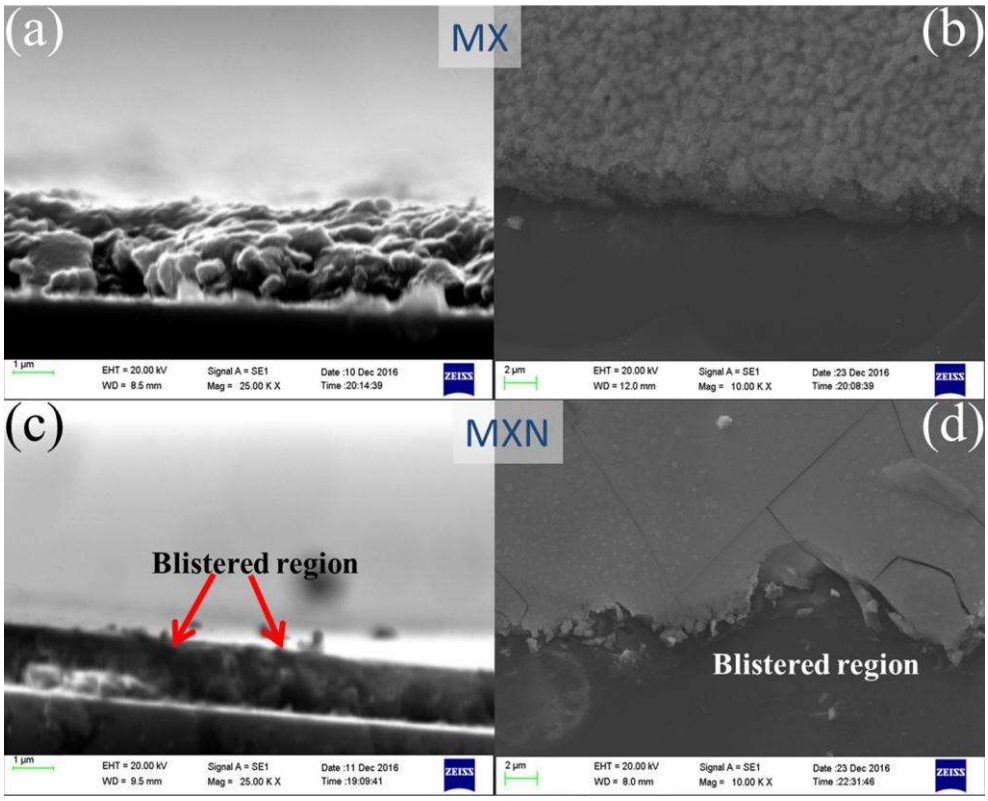

Figure 4.7 Cross-sectional SEM micrographs for 300 °C annealed (a) chloride sol derived (MX) (b) Nitrate sol derived (MXN) CZTS thin films and corresponding surface morphology (c) chloride sol derived (MX) (d) Nitrate sol derived (MXN)

The diffuse reflectance data are collected in 300-900 nm wavelength range to understand the optical response of these films. This reflectance is used to calculate spectral absorptance using Kubelka-Munk model $F(R) = \frac{(100-R)^2}{2R}$; where F(R) is Kubelka-Munk function and R is the percent diffuse reflectance. The calculated F(R) has been used to calculate the optical band gap of the material using Tauc relation $(\alpha h\nu)^{1/n} = A(h\nu - Eg)$ where α is absorption coefficient, h is Plank's constant, ν is photon frequency, A is proportionality constant and E_g is band gap of the material. The exponent n in the Tauc relation signifies the nature of optical band gap. The value of n equal to $1/2$, $3/2$, 2 and 3 corresponds to direct allowed, direct forbidden, indirect allowed and indirect forbidden transitions respectively [Viezbicke, Patel, Davis, & Birnie, 2015]. Considering CZTS a direct bandgap material $(F(R)h\nu)^2$ with respect to energy hν is plotted and shown in **Figure 4.8 (a, b)**.The bandgap of the prepared film is obtained by extrapolating the linear region in the plot and found a bandgap of ~ 1.52 eV for both chloride and nitrate sol derived CZTS films.

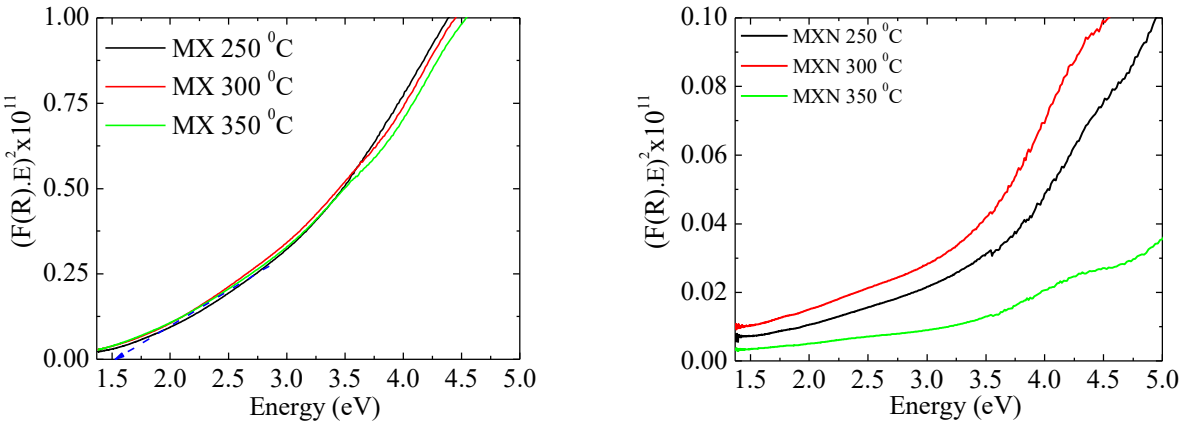

Figure 4.8 (α.E) ² vs. photon energy plot for CZTS thin films processed at different annealing temperature using a) Chloride sol b) Nitrate sol

The optical measurements are also carried out for different temperature annealed CZTS thin films and are shown in **Figure 4.8**. We found that there is no significant change in optical bandgap for CZTS films prepared using chloride sols while small decrease in bandgap is noticed for nitrate sol derived CZTS films annealed at higher temperatures. In addition to this, CZTS film prepared using nitrate sol showed an order of magnitude smaller absorption than chloride route prepared CZTS films, which further decreased for films annealed at higher temperatures, **Figure 4.8 (b)**. Other optical parameters such as refractive index (n) and dielectric constant (ε_∞)are calculated using modified Moss relation $E_g n^4 = 108\, eV$ [P. Gupta & Ravindra, 1980]. The static dielectric constant (ε_{static}) and high frequency dielectric constant (ε_∞) are calculated using the relations $\varepsilon_{static} = 18.52 - 3.08\, E_g$ and $\varepsilon_\infty = n^2$ [Henry, Mohanraj, & Sivakumar, 2015]. The calculated values of n, ε_{static}, ε_∞ for CZTS thin film corresponding to band gap value of 1.52 eV are 2.90, 13.84, and 8.43, respectively. These values are consistent with other reports [Henry et al., 2015].

In electrical characterization room temperature resistivity measurements are carried out in van der Pauw configuration at different positions across 1′ x 1′ CZTS thin films. CZTS thin film processed at 300 °C with both chloride and nitrate sol are taken for the resistivity mapping and results are shown in **Figure 4.9** as this temperature resulted in relatively better CZTS thin film structure as compared to other different temperature processed CZTS films. The obtained resistivity mapping across the films suggests uniform resistivity distribution for films prepared using chloride sol as compared to that of nitrate sol derived CZTS film.

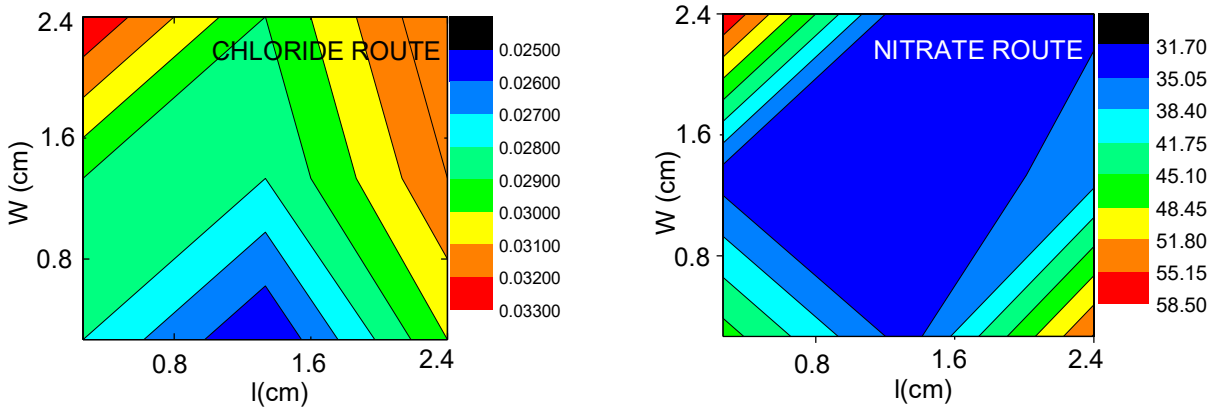

Figure 4.9 van der Pauw resistivity mapping of CZTS thin film across 1 inch x 1 inch glass substrate prepared using a) Chloride sol and b) Nitrate sol after 300 °C annealing

The chloride sol derived film shows lower resistivity with very small variation 0.025 ± 0.008 Ωcm across whole surface of the film. However, nitrate sol derived CZTS shows large resistivity with very high variation 31.70 ± 26.2 Ωcm which confirms the presence of non-uniformity and defects in the films as confirmed by the SEM measurements. Current –voltage (I-V) characteristics are collected in two points configurations on the surface of the film and are shown in **Figure 4.10** for both CZTS film processed at 300 °C using chloride sol and nitrate sols. These measurements suggest that chloride sol derived CZTS film is less resistive and the resistivity further decreases with increase in temperature as shown in inset of **Figure 4.10 (a)**. Nitrate sol derived CZTS shows opposite trend and their resistivity increases with increase in processing temperature as shown in inset of **Figure 4.10 (b)**. This increase in resistivity in spite of increasing the grain size, with increase in processing temperature is possibly due to the increased defects such as cracks and blisters which may form discontinuity across the film and restrict the current flow.

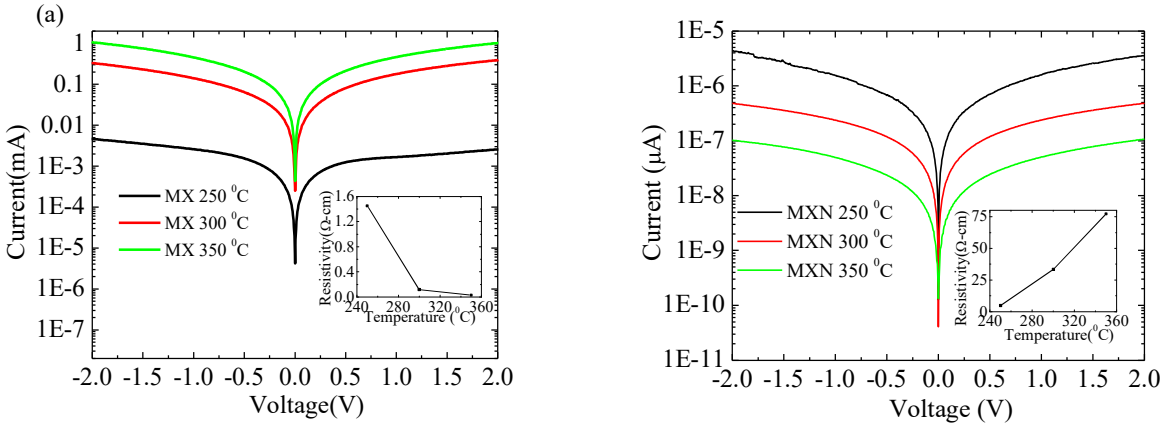

Figure 4.10 Current-voltage characteristics of CZTS thin films prepared using (a) Chloride sol b) Nitrate sol at different temperature. Inset in both the graph represents room temperature resistivity of the films with processing temperature measured using van der Paw configuration.

4.5 Conclusion

Two different set of metal salts have been investigated to prepare a stable sol suitable for spin coating to grow CZTS thin film. The observed results suggest that chloride sol is relatively better as compared to that of nitrate sol for spin coating. A uniform, dense and phase pure CZTS thin film has been grown using spin coating and post annealing at lower temperature (300 °C)under air ambient conditions. A uniform resistivity distribution and good electrical response

across the films are achieved for chloride sol derived CZTS thin films. As this process does not require any additional sulfurization steps at higher temperature, it can be further extended to fabricate heterostructure solar cell devices. This method has flexibility that property of the grown CZTS thin film can be easily tailored by changing the composition of the sol or by changing the annealing conditions. Any kind of intentional doping is easily possible in this method and can be further optimized to make large area CZTS film for photovoltaic application.